ISSN 1807-1929
Revista Brasileira de Engenharia Agrícola e Ambiental
v.22, n.9, p.591-596, 2018
Campina Grande, PB, UAEA/UFCG – http://www.agriambi.com.br

DOI: http://dx.doi.org/10.1590/1807-1929/agriambi.v22n9p591-596

Abrasive effects of sediments on impellers of pumps used for catching raw water

Rodrigo O. P. Serrano[1], Ana L. P. de Castro[1], Edwin A. M. Rico[1], Maria A. Pinto[2], Edna M. de F. Viana[1] & Carlos B. Martinez[1]

[1] Universidade Federal de Minas Gerais/Programa de Pós-Graduação em Engenharia Mecânica. Belo Horizonte, MG. E-mail: ropereas@gmail.com (Corresponding author) - ORCID: 0000-0002-7786-8305; analeticiapilz@gmail.com - ORCID: 0000-0003-3842-2519; eng.andresmancilla@gmail.com - ORCID: 0000-0002-5133-0283; ednamariafaria@bol.com.br - ORCID: 0000-0002-3853-1355; martinez@cce.ufmg.br - ORCID: 0000-0002-0653-5298
[2] Universidade Federal de Ouro Preto/Escola de Minas. Ouro Preto, MG. E-mail: mariap06@gmail.com - ORCID: 0000-0003-1208-2210

Key words:
abrasive wear
micro abrasion
sediment concentration

ABSTRACT
This study presents an analysis of the abrasive effects of sediments from the bed of the Acre River, Brazil, on the wear of three different ferrous materials employed in the manufacture of impellers of centrifuge pumps used to catch raw water. In order to evaluate the abrasive wear and specific wear coefficient (k) as a function of sediment concentration, tests were conducted in samples of SAE 8620 steel, nodular cast iron and gray cast iron by using a rotary-ball abrasion meter. These tests employed abrasive slurry with concentration of 1, 2, 3, 5 and 10 g L^{-1} of sediments in distilled water. The volume of worn material as a function of the relative velocity of water flow in relation to the impeller blades was mathematically estimated. The experimental results showed that: i) The semi-angular and semi-rounded shapes of the sediments from the Acre River produced evidence of micro-grooving and plastic deformation in the three metallic alloys; ii) SAE 8620 steel showed higher resistance to abrasive wear than samples of gray and nodular cast iron; iii) the increase in the volume of worn material due to increment in sediment concentration and the relative velocity of the mixture (water + sediment) to the rotor pads.

Palavras-chave:
desgaste abrasivo
microabrasão
concentração de sedimentos

Efeitos abrasivos dos sedimentos em rotores de bombas utilizadas na captação de água bruta

RESUMO
Neste estudo analisou-se a capacidade abrasiva dos sedimentos do leito do Rio Acre, Brasil, no desgaste de 3 materiais ferrosos diferentes utilizados na fabricação de rotores de bombas centrífugas, utilizados na captação de água bruta. Para determinar o modo de desgaste e a relação do coeficiente de desgaste específico do material (k), em função da concentração de sedimentos, foram realizados ensaios em abrasômetro de esfera rotativa em amostras de aço SAE 8620, ferro fundido nodular e em ferro fundido cinzento, usando como suspensões abrasivas as concentrações de 1, 2, 3, 5 e 10 g L^{-1} de sedimento em água destilada. O volume de desgaste em função da velocidade relativa do fluxo da água em relação às pás do rotor foi estimado matematicamente. Os resultados mostraram que: i) As formas semiangulares e semiarredondadas dos sedimentos do Rio Acre produziram evidencias de microssulcamento e deformação plástica nas três ligas metálicas; ii) O aço SAE 8620 mostrou maior resistência ao desgaste abrasivo do que as amostras de ferros fundidos cinzento e nodular; e iii) O aumento do volume de desgaste decorrente da aumento da concentração de sedimento e da velocidade relativa que a mistura (água + sedimento) para pelas pás do rotor.

Ref. 185967 – Received 02 Oct, 2017 • Accepted 30 Apr, 2018 • Published 25 Jul, 2018

Introduction

Pumps used for catching raw water, installed in rivers of sedimentary waters intended for projects of irrigation and urban and rural supply, undergo wear on impellers caused by the abrasion of the sediments in suspension. According to Xing et al. (2009), diameter and concentration of sediment particles have great influence on the wear conditions of centrifuge pumps, causing points of deformation resulting from the impact of particles on the surface of the impeller blades.

Maio et al. (2012), analyzing the wear in the presence of solids in suspension in centrifuge pumps, concluded that the increase in vibration, resulting from the erosion caused by the abrasion of the sediments, may indicate an evolution in pump wear and is the main cause of the reduction in its efficiency and useful life.

Upadhyay & Kumaraswamidhas (2014) also highlight that it is important to know the characteristics of the abrasive agent to subsequently verify the alternatives to improve the resistance to wear.

In centrifuge pumps, wear by abrasion occurs between the impeller and stationary cover of the casing, between the shaft and stationary casing and, mainly, on the surface of impeller blades, possibly causing imbalance and losses of efficiency (Maio et al., 2012).

In this context, this study aimed to understand the behavior of micro-abrasive wear caused by different concentrations of fluvial sediments in 3 metallic alloys used in the manufacture of centrifuge pump impellers, and estimate the variation in wear as a function of the relative velocity at which the mixture (water + sediment) passes through the impeller blades.

Material and Methods

Since there are various manufacturers and models of pumps that can be used to catch raw water, we opted for using construction characteristics of a project impeller, according to the methodology described by Macintyre (2013).

In the present study, the flow rate (Q) range was adopted to supply an irrigation system for rural properties of the order of 30 to 60 L h^{-1}, with manometric height (H) of 40 m and rotation (n) of 3500 rpm. To aid in the calculations, we used algorithms developed by Palomino (2017), which use the specific rotation (nq), given by Eq. 1, to indicate the main characteristics of an impeller and the velocity triangles at the inlet and outlet of the blades.

$$nq = n\frac{Q^{1/2}}{H^{3/4}} \quad (1)$$

Based on the velocity triangle, the relative velocity of the fluid was determined when it tangentially passes by the blades at the impeller inlet and outlet. This velocity was used to calculate the abrasive fluid's drag force as a function of the relative velocity, described in Eq. 2 (Fox et al., 2006).

$$F_D = \frac{C_D\ \rho\ V^2\ A}{2} \quad (2)$$

where:

F_D - drag force, N;
C_D - drag coefficient, dimensionless;
A - area, m^2;
ρ - fluid density, kg m^{-3}; and,
V - fluid velocity, m s^{-1}.

Considering that the flow is laminar at the beginning of the blade, changing to turbulent, the drag coefficient was determined using Eq. 3, which takes into account the change in flow regime (Fox et al., 2006).

$$C_D = \frac{0.0742}{Re^{(0.2)}} - \frac{1740}{Re} \quad (3)$$

and Reynolds number (Re) is given by Eq. 4:

$$Re = \frac{DV}{\nu} \quad (4)$$

where:

V - velocity, m s^{-1};
D - distance from the blade, m; and,
ν - kinematic viscosity, m^2 s^{-1}.

The analyzed samples were of gray cast iron (GCI), nodular cast iron (NCI) and SAE 8620 steel, with hardness of 60, 62 and 80 HRA, respectively, and the materials are similar to the metallic alloys used in impeller manufacture.

Chemical analyses of the metallic alloys were carried out in optical emission spectrophotometer (Table 1). The samples were filed, polished and cleaned to eliminate scratches, oxidations and deeper marks on the surface which could interfere with the test and analysis of the craters in Scanning Electron Microscope (SEM).

The origins of the sediments in suspension are related to the geomorphological dynamics of the rivers, resulting from erosive processes which are intensified in the rainy season. In this case, the sediments used come from the Acre River waters, which wet the geological units of the Solimões Formation and its alluvial terraces, collected at the coordinates 10° 1' 1" S and 67° 50' 52" W, upstream of the urban area of the Rio Branco city, in the state of Acre.

The sediments were classified as sandy, fine, angular with little sphericity, composed of quartz, feldspars, smectite, illite and kaolinite, with D50 of 0.097 mm (Figure 1), and 74% of the sample was composed of quartz sand.

Table 1. Chemical composition of the metallic alloys (% in weight)

Alloy	C	Si	S	P	Mn	Cu	Cr
GCI	2.742	2.581	0.029	0.103	0.143	0.035	0.042
NCI	3.697	2.922	0.006	0.026	0.210	0.048	0.018
	C	**Si**	**S**	**Mn**	**Cr**	**Ni**	**Mo**
SAE 8620 steel	0.766	0.264	0.013	0.782	0.461	0.495	0.167

GCI – Gray cast iron; NCI – Nodular cast iron

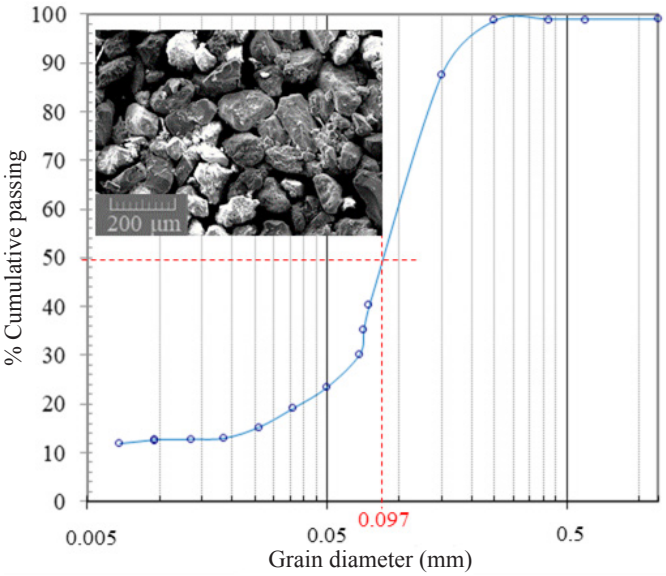

Figure 1. Granulometric distribution and Scanning Electron Microscope (SEM) micrograph of sediment particles

After analyzing four types of abrasive wear methods cited in the literature (Ahmadian et al., 2005; Itoi et al., 2010; Malafaia et al., 2010; Gant & Gee, 2011; Fernandes et al., 2012; Cozza et al., 2015; Farfán-Cabrera et al., 2016), it was verified that the method of rotary ball on plate, or micro-abrasion by rotary ball, provides favorable conditions for the abrasiveness analysis of sediments in metallic alloy samples.

In this test, a wear crater is formed on sample surface (Figure 2), allowing the calculation of worn volume (Qw) of a material with hardness (H_T) based on crater diameter.

During the tests a normal force is applied on the sample and a tangential force is applied on the abrasive particles due to the rotation of the ball, which enable the abrasive particles to penetrate, scratch and remove material from the sample, forming a wear crater.

Wear coefficient is calculated based on the volume of material removed during the test, using Eq. 5 (Rutherford & Hutchings 1997; Allsopp & Hutchings, 2001; Santos et al., 2015; Krelling et al., 2017).

$$k = \frac{\pi D^4}{64 R S F_N} \quad (5)$$

where:

k - wear coefficient, $m^3 N^{-1} m^{-1}$;
D - crater diameter, m;
R - crater radius, m;
S - sliding distance, m; and,
F_N - normal force applied, N.

The tests were conducted at the Micro-abrasion Laboratory of the Federal University of Ouro Preto (UFOP). During the procedures, an AISI 52100 Steel ball with 25 mm diameter was used at 100 rpm rotation, 180 m sliding distance, 3 N load applied on the sample (F_N) and abrasive slurries composed of sediments at concentrations of 1, 2, 3, 5 and 10 g L^{-1}, in distilled water.

The tests were conducted in triplicate and the craters generated on the samples were analyzed using SEM images

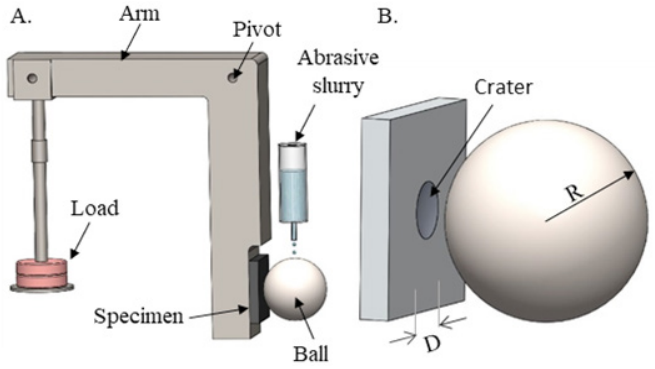

Figure 2. Diagram of the test device (A) and spherical crater produced by abrasive wear on the sample (B)

of the NANOLAB of UFOP, which allowed the determination of crater diameter and analysis of wear surfaces to determine the acting wear mechanism. The obtained data allowed the comparison of the wear produced as a function of the variation in sediment concentration.

To estimate the volume of metallic material loss in the impellers manufactured with the same metallic alloys the Archard equation (Eq. 6) given by Santos et al. (2015) was used:

$$Q_W = \frac{K}{H_m} F_N S \quad (6)$$

where:

Q_W - volume of material worn, m^3;
K - wear severity, dimensionless;
H_m - material hardness, N mm^{-2};
F_N - normal force applied, N; and,
S - sliding distance, m.

Considering that (K) is a dimensionless constant, which will be divided by the hardness of the worn material (H), and that (k) in Eq. 5 refers to a specific wear coefficient of a material, Eq. 6 was adjusted and the volume of material worn (Q_W) was obtained as shown in Eq. 7:

$$Q_W = k F_D S \quad (7)$$

where:

Q_W - volume of material worn, m^3;
k - wear coefficient of the material, $m^3 N^{-1} m^{-1}$;
F_D - drag force acting on a $1cm^2$ area on the blade, N; and,
S - relative sliding distance of the blade, m.

Considering the relative velocity of the mixture (water + sediment) passing through a certain area of the impeller blade, a relative sliding distance (S) was estimated according to Eq. 8:

$$S = V t \quad (8)$$

where:

V - relative velocity of the fluid passing through the blade, m s^{-1}; and,
t - time of pump operation, s.

The force F_D, considered in Eq. 7, was calculated using Eq. 2 based on the abrasive drag force which can occur on 1 cm² area of the blade surface.

Results and Discussion

The diameters of the craters generated in the wear tests for the studied sediment concentrations were used to calculate the wear coefficient (k) using Eq. 5.

To evaluate the relationship between wear coefficient and sediment concentration in the abrasive slurry, curves were created for the materials analyzed (Figure 3). It was observed that the wear coefficient 'k' increased with the increment in sediment concentration, at constant values of 'F_N' and 'S', which can be related to a higher number of particles in the specimen/ball contact, resulting in greater wear (Trezona et al., 1999; Pintaúde, 2002; Cozza, 2011; Krelling et al., 2017).

Worn volume variation as a function of abrasive concentration had the same behavior for the three materials analyzed (Figure 3). Furthermore, for SAE 8620 steel, with higher hardness (80 HRA), the effect of increased abrasive concentration is smaller on the wear coefficient.

It is important to point out that, during the tests, the type of wear did not change as a function of the variation in sediment concentration, since the concentrations were not higher than 18% (Cozza, 2011), justifying the coherence of the logarithmic curve with R^2 close 1.

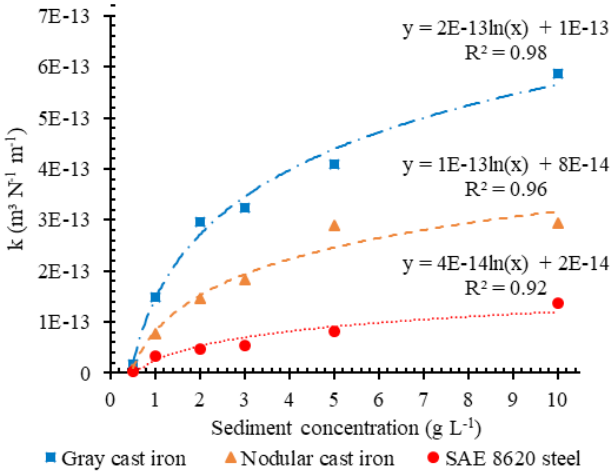

Figure 3. Behavior of the specific wear coefficient (k) as a function of the variation in sediment concentration, for the test conditions described in the methodology (S = 180 m and F_N = 3 N)

The values of 'k' for the concentrations of 0.5 g L^{-1}, presented in the graph of Figure 3, were calculated using the logarithmic curve equation, generated by the experimental wear data, for the concentrations of 1, 2, 3, 5 and 10 g L^{-1}.

According to the images obtained through SEM (Figure 4), the craters created in the tests demonstrated the predominant action of micro-grooving or two-body wear for the 3 metallic alloys analyzed, with clear direction. No changes were

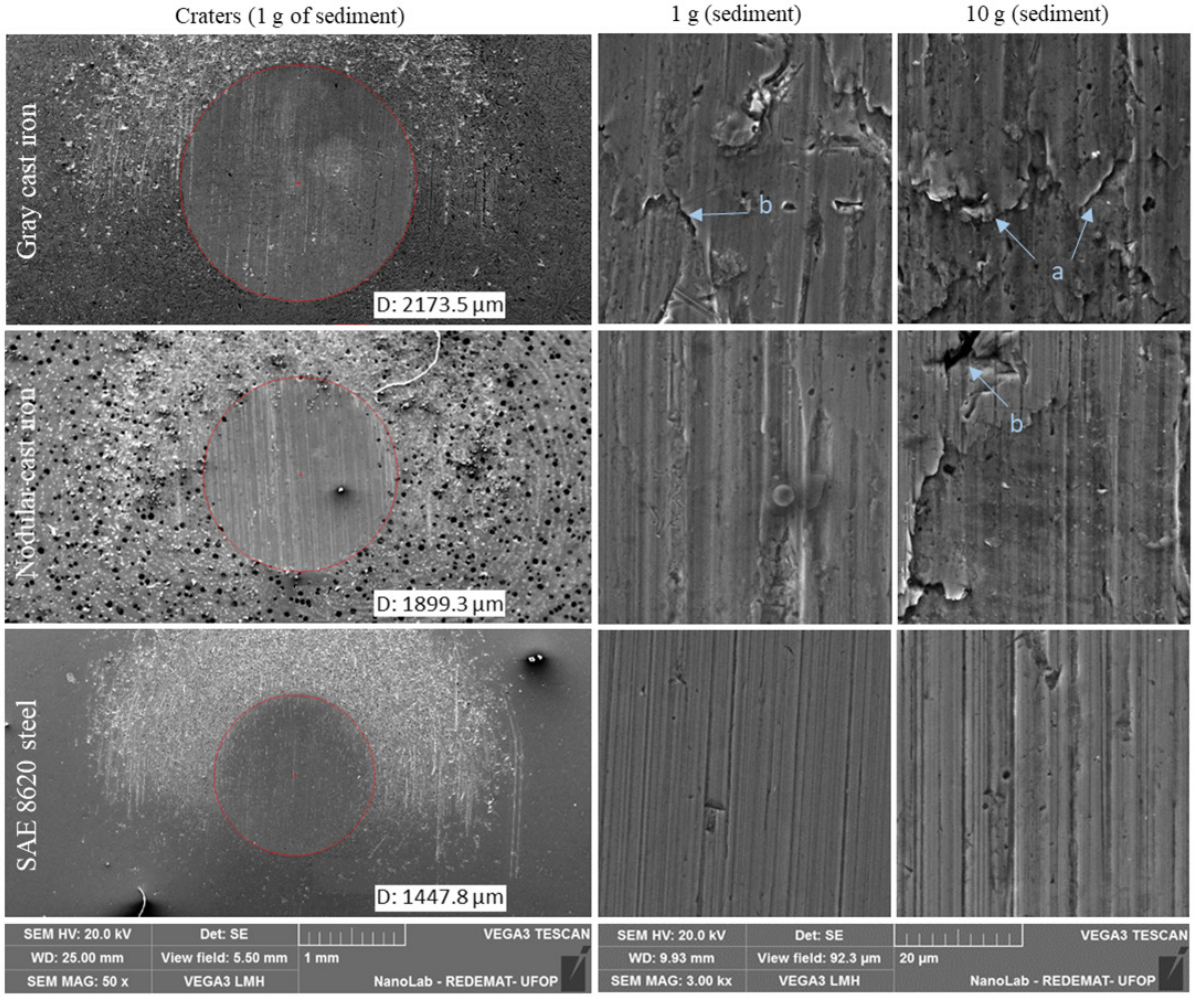

Figure 4. Type of abrasive wear resulting from the tests with rotary-ball abrasion meter with F_N = 3 N

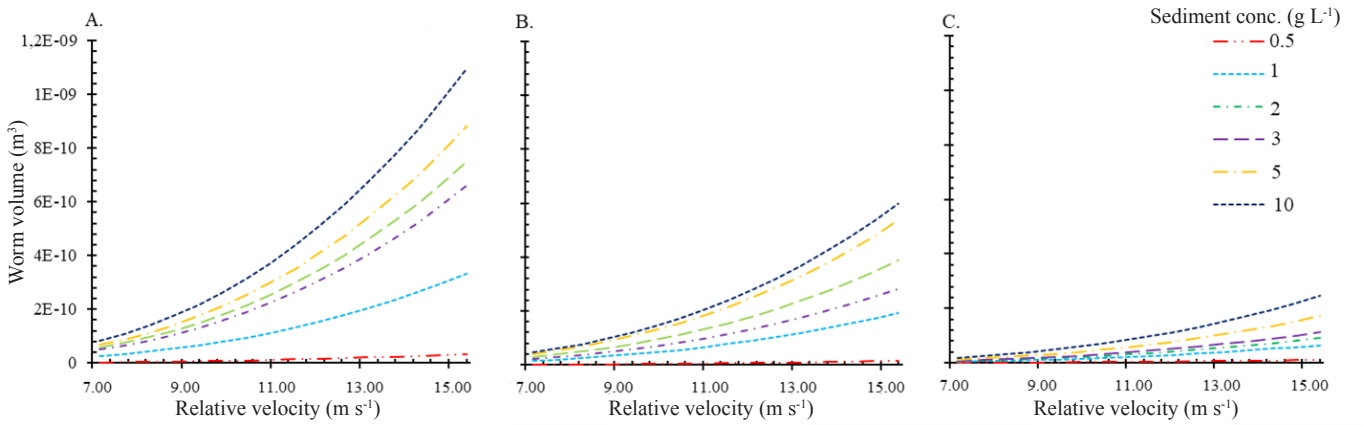

Figure 5. Numerical estimate of worn volume as a function of relative velocity of the mixture and sediment concentration (g L^{-1}), for 1 cm^2 of blade within 1 hour of operation: (A) Gray cast iron, (B) Nodular cast iron and (C) SAE 8620 steel

observed in the wear mechanism with the increase in abrasive concentration, demonstrating that it is an adequate technique to investigate the abrasive capacity of the sediments and wear of the iron alloys used.

These results are consistent with those presented in the literature, in which micro-grooving wear is favored by F_N >1 N and abrasive material concentrations below 18% (Trezona et al., 1999; Adachi & Hutchings, 2005; Cozza, 2013).

The specimens of gray and nodular cast irons had areas with plastic deformation, more evident in the gray cast iron. In this case, micro-grooving is associated with the plastic deformation, accumulation of materials on groove edges, and intensification due to the increase in sediment concentration.

The material accumulated on groove edges is later removed due to the association of the micro-grooving mechanism with low-cycle fatigue mechanisms, as observed by Pintaúde (2002). For gray cast iron, there is an accumulation of material also in front of the worn grooves (Figure 4: point a). In addition, points where material removal caused by incrustation and subsequent removal of abrasive particles were observed in gray and nodular cast irons (Figure 4: point b), which led to increase in their wear rates.

The velocity fields found for the project impellers, at the required demand, varied from 7.17 to 15.40 m s^{-1}. Considering a mean impeller blade length of 87 mm, the effects of wear on the impeller were estimated as a function of the velocity at which the mixture passes through the impeller blades (Figure 5).

It is possible to note in Figure 5 that the highest resistance to abrasive wear was obtained by the SAE 8620 steel, which was 500% more resistant than gray cast iron and 295% more resistant than nodular cast iron, for concentrations of 1 g L^{-1}. Comparing both cast irons, it is observed that nodular cast iron was 170% more resistant to abrasive wear than gray cast iron, for the same sediment concentration.

The difference in volume of worn material between cast irons can be related to the microstructure of the alloys, since nodular cast iron is more ductile than gray cast iron.

Considering that the relative velocity was determined using Eq. 1, i.e., as a function of Q (system supply flow rate), H (manometric height) and n (impeller rotation), surveying these data could guide the selection of the best motor pump set in order to have lower relative velocities. Variation of sediment concentration in the river along the year should be considered to evaluate the cost-benefit ratio of the different metallic alloys used in the manufacture of impellers. As shown in Figures 4 and 5, SAE 8620 steel had higher resistance to abrasive wear but is more expensive than the cast irons.

Conclusions

1. The semi-angular and semi-rounded shapes of the sediments from the Acre River produced evidences of micro-grooving and plastic deformation in the three metallic alloys at all sediment concentrations used in the tests.

2. The abrasive capacity of the sediments was evident in the worn craters of the three metallic alloys and was less intense in SAE 8620 steel, due to its higher hardness (70 HRA).

3. The estimation of wear as a function of increasing sediment concentration and relative velocity of the mixture (water + sediment) showed exponential increase in worn volume.

4. The analysis of worn volume, as a function of the type of metallic alloy, sediment concentration and relative velocity in the impellers demonstrated the importance of a previous study on the concentration of sediments in the sources of waters used in irrigation and on distance from this source to the reservoir and the required flow rate, to select the best motor pump set.

Acknowledgments

The authors express their gratitude to the Gorceix Foundation, ANEEL, CEMIG, ELETROBRAS-FURNAS, FAPEMIG, CNPq and CAPES for the financial aid to the study, and to the LTM, NANOLAB and UFOP's Micro-abrasion Laboratories and to the CPH of the UFMG for the support in the conduction of the tests.

Literature Cited

Adachi, K.; Hutchings, I. M. Sensitivity of wear rates in the micro-scale abrasion test to test conditions and material hardness. Wear, v.258, p.318-321, 2005. https://doi.org/10.1016/j.wear.2004.02.016

Ahmadian, M.; Wexler, D.; Chandra, T.; Calka, A. Abrasive wear of WC-FeAl-B and WC-Ni3Al-B composites. International Journal of Refractory Metals & Hard Materials, v.23, p.155-159, 2005. https://doi.org/10.1016/j.ijrmhm.2004.12.002

Allsopp, D. N.; Hutchings, I. M. Micro-scale abrasion and scratch response of PVD coatings at elevated temperatures. Wear, v.251, p.1308-1314, 2001. https://doi.org/10.1016/S0043-1648(01)00755-4

Cozza, R. C. Estudo do desgaste e atrito em ensaios micro-abrasivos por esfera rotativa fixa em condições de força normal constante e pressão constante. São Paulo: Escola Politécnica da USP, 2011. 327p. Tese Doutorado. https://doi.org/10.11606/T.3.2011.tde-26082011-143752

Cozza, R. C. Effect of pressure on abrasive wear mode transitions in micro-abrasive wear tests of WC-Co P20. Tribology International, v.57, p.266-271, 2013. https://doi.org/10.1016/j.triboint.2012.06.028

Cozza, R. C.; Rodrigues, L. C.; Schon, C. G. Analysis of the micro-abrasive wear behavior of an iron aluminide alloy under ambient and high-temperature conditions. Wear, v.330-331, p.250-260, 2015. https://doi.org/10.1016/j.wear.2015.02.021

Farfán-Cabrera, L. I.; Gallardo-Hernández, E. A.; Pascual-Francisco, J. B.; Resendiz-Calderon, C. D.; Rosa, C. S. de la. Experimental method for wear assessment of sealing elastomers. Polymer Testing, v.53, p.116-121, 2016. https://doi.org/10.1016/j.polymertesting.2016.04.021

Fernandes, F.; Ramalho, A.; Loureiro, A.; Cavaleiro, A. Mapping the micro-abrasion resistance of a Ni-based coating deposited by PTA on gray cast iron. Wear, v.298, p.151-158, 2012. https://doi.org/10.1016/j.wear.2012.05.018

Fox, R. W.; McDonald, A. T.; Pritchard, P. J. Introdução à mecânica de fluidos. 6.ed. Rio de Janeiro: LTC, 2006. 798p.

Gant, A. J.; Gee, M. G. A review of micro-scale abrasion testing. Journal of Physics D: Applied Physics, v.44, p.1-15, 2011. https://doi.org/10.1088/0022-3727/44/7/073001

Itoi, T.; Mineta, S.; Kimura, H.; Yoshimi, K.; Hirohashi, M. Fabrication and wear properties of Fe_3Al-based composites. Intermetallics, v.18, p.2169-2177, 2010. https://doi.org/10.1016/j.intermet.2010.07.014

Krelling, A. P.; Costa, C. E. da; Milan, J. C. G.; Almeida, E. A. S. Micro-abrasive wear mechanisms of borided AISI 1020 steel. Tribology International, v.111, p.234-242, 2017. https://doi.org/10.1016/j.triboint.2017.03.017

Macintyre, A. J. Bombas e instalações de bombeamento. 2.ed. Rio de Janeiro: LTC, 2013. 782p.

Maio, F. di; Hu, J.; Tse, P.; Pecht, M.; Tsui, K.; Zio, E. Ensemble-approaches for clustering health status of oil sand pumps. Expert Systems with Applications, v.39, p.4847-4859, 2012. https://doi.org/10.1016/j.eswa.2011.10.008

Malafaia, A. M. S.; Milan, M. T.; Omar, M.; Riofano, R. M. M.; Oliveira, M. F. de. Oxidation and abrasive wear of Fe–Si and Fe–Al intermetallic alloys. Journal of Materials Science, v.45, p.5393-5397, 2010. https://doi.org/10.1007/s10853-010-4591-4

Palomino, A. E. C. Desenvolvimento de metodologia para determinação dimensional de uma bomba centrífuga utilizando velocidades específicas (ns). Belo Horizonte: UFMG, 2017. 132p. Dissertação Mestrado

Pintaúde, G. Análise dos regimes moderado e severo de desgaste abrasivo utilizando ensaios instrumentados de dureza. São Paulo: Escola Politécnica da USP, 2002. 200p. Tese Doutorado. https://doi.org/10.11606/T.3.2002.tde-07042010-111922

Rutherford, K. L.; Hutchings I. M. Theory and application of a micro-scale abrasive wear test. Journal of Testing Evaluation of the American Society for Testing and Materials, v.25, p.250-260, 1997. https://doi.org/10.1520/JTE11487J

Santos, W. C.; Pereira Neto, J. O.; Silva, R. O.; Rodriguês, G.; Moreto, J. A.; Manfrinato, M. D.; Rossino, L. S. Desenvolvimento de dispositivo e estudo do comportamento ao micro desgaste abrasivo do aço AISI 420 temperado e revenido. Revista Matéria, v.20, p.304-315, 2015. https://doi.org/10.1590/S1517-707620150002.0031

Trezona, R. I.; Allsopp, D. N. Hutchings, I. M. Transitions between two-body and three-body abrasive wear: Influence of test conditions in the microscale abrasive wear test. Wear, v.225, p.205-214, 1999. https://doi.org/10.1016/S0043-1648(98)00358-5

Upadhyay, R. K.; Kumaraswamidhas, L. A. A review on tribology of surfaces and interfaces. Advanced Materials Letters, v.5, p.486-495, 2014. https://doi.org/10.5185/amlett.2014.5566

Xing, D.; Hai-Lu, Z.; Xin-Yong, W. Finite element analysis of wear for centrifugal slurry pump. In: International Conference on Mining Science and Technology, 6, 2009, China. Proceedings… China: Procedia Earth and Planetary Science, 2009. p.1532-1538. https://doi.org/10.1016/j.proeps.2009.09.236